

Corrosion Inhibition of Carbon Steel by Imidazolium and Pyridinium Cations Ionic Liquids in Acidic Environment

Magdy A.M. Ibrahim,^{*,1,2} Mouslim Messali,¹ Ziad Moussa,¹ Abdullah Y. Alzahrani,¹ Saleh N. Alamry,³ Belkheir Hammouti⁴

¹Chemistry Department, Faculty of Science, Taibah University, Al Madinah Al Mounawara, 30002 Saudi Arabia

²Chemistry Department, Faculty of Science, Ain Shams University, Abbassia, Cairo, Egypt

³Physics Department, Faculty of Science, Taibah University, Al Madinah Al Mounawara, 30002 Saudi Arabia

⁴LCAE-URAC18, Faculté des Sciences, Université Mohamed Premier, B.P. 4808, 60046 Oujda, Morocco

Received 11 April 2011; accepted 25 November 2011

Abstract

New imidazolium-based ionic liquids and some pyridinium-based ionic liquids, were tested as corrosion inhibitors of steel in 1.0 M HCl using potentiodynamic polarization, linear polarization and weight loss methods. The obtained results showed that all of the four ILs are good inhibitors for steel in 1.0 M HCl and the inhibition efficiency increased with increasing the inhibitor concentration. All of the ILs act as mixed-type inhibitors. Obtained results from Tafel polarization, linear polarization and weight loss are in good agreement with each other. The adsorption of the four ILs inhibitors, obey the Langmuir adsorption isotherm. From the adsorption isotherm, values of ΔG_{ads} for the adsorption process were calculated. The effect of temperature on the corrosion behavior of steel in presence of 1×10^{-3} M of compound II was studied in the temperature range 298-338 K.

Keywords: corrosion inhibitor, electrochemical techniques, ionic inhibitor, adsorption.

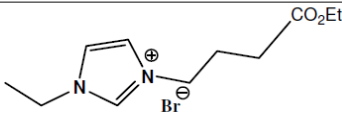
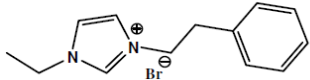
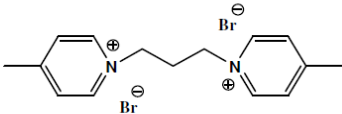
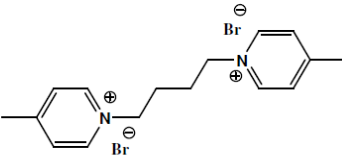
Introduction

Acid solutions are widely used in industrial acid cleaning, acid descaling, acid pickling, and oil well acidizing, requiring the use of corrosion inhibitors in order to minimize their corrosion attack on metallic materials. The use of organic compounds containing oxygen, sulfur and especially nitrogen, to reduce

* Corresponding author. E-mail address: imagdy1963@hotmail.com

corrosion attack on steel has been studied in some details [1-7]. The development of new corrosion inhibitors of non-toxic nature, which do not contain heavy metals and organic phosphates, is very important [8]. The inhibitors can decrease the dissolution rate of metals in acids, affecting the kinetics of the electrochemical reactions which constitute the corrosion process. Adsorption of inhibitor on the metal surface will change the structure of the electric double layer. The adsorption itself depends to a great extent on the molecular structure. Previous investigations showed that the inhibition efficiency is improved predominantly by increasing the molecular surface area and influenced by the position of the substituents as well [9-11]. For planar molecules with very similar molecular surface areas the adsorption properties are also function of the electronic structure of the molecule [12].

Table 1. Ionic liquids.

Compound	Structural formula	Molar mass
I		291.18
II		281.19
III		388.14
IV		402.17

Although ILs are expected to be good candidates as corrosion inhibitors because of their environmentally friendly characteristics in addition to their unique properties [13-15], little investigations have been found in literature [16,17]. Zhang et al. [18] have investigated the behavior of alkyimidazolium ionic liquids for steel in acidic medium. It was found that ILs exhibited excellent inhibition performance for mild steel in acidic solution. Imidazolium compounds are reported to show corrosion resistant behavior of copper [19], steel [20, 21] and aluminum [22]. It is found that the action of such inhibitors depends on the specific interaction between the functional groups and the metal surface, due to the presence of the $-C=N-$ group and electronegative nitrogen in the molecule. The objective of the present work was to study the applicability of four ILs namely: 3-(4-ethoxy-4-oxobutyl)-1-ethylimidazol-3-ium bromide (I) and 1-ethyl-3-phenethylimidazol-3-ium bromide (II), 1,1'-(propane-1,3-diyl)bis(4-methylpyridinium)dibromide (III), and 1,1'-(butane-1,4-diyl)bis(4-methylpyridinium)dibromide (IV), as corrosion inhibitors for carbon steel in 1.0 M HCl (Table 1). It

is also aimed to predict the thermodynamic feasibility of adsorption of the ILs inhibitor molecules on steel surface and to study their adsorption behavior.

Experimental methods

Chemical synthesis

Materials

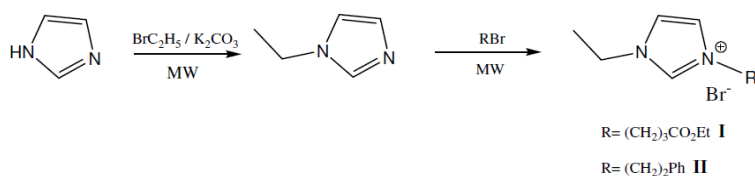
The reagents: imidazole (99%), ethyl 4-bromo butyrate (96%), (2-bromoethyl)benzene, 4-picoline, 1,3-dibromopropane and 1,4-dibromobutane were purchased from Aldrich and used as received. All solvents were of HPLC grade.

Measurements and equipments

All new compounds were synthesized and characterized by ^1H NMR and ^{13}C NMR spectroscopies. ^1H NMR (400 MHz) and ^{13}C NMR (100 MHz) spectra were obtained in DMSO at room temperature. Chemical shifts (δ) were reported in ppm to a scale calibrated for tetramethylsilane (TMS), which is used as an internal standard. The LCMS spectra were measured with a Micromass, LCT mass spectrometer. The microwave-assisted reactions were performed using a controllable single-mode microwave reactor, CEM Discovery, designed for synthetic use. The reactor is equipped with a magnetic stirrer as well as a pressure, temperature and power controls. The maximum operating pressure of the reactor is 20 bar. The power and temperature range are 15-300 W and 60–250 °C, respectively.

Microwave assisted synthesis of imidazolium ionic liquids

New environmentally friendly imidazolium-based ionic liquids, **I** and **II**, were prepared for the first time by using microwave irradiation in short duration of time with quantitative yields.



Scheme 1. N-alkylation of N-ethylimidazole under microwave irradiation (MW).

3-(4-ethoxy-4-oxobutyl)-1-ethylimidazol-3-ium bromide (I)

N-ethylimidazole (1 g, 0.0104 mol) and ethyl 4-bromobutyrate (2.03 g, 0.0104 mol) and 10 mL of toluene were placed in a microwave reactor vessel and irradiated for 20 minutes at 100 °C. The crude product was washed a few times with dry ethyl acetate and dried overnight in a vacuum at 70 °C. The yield of **I** was 92%. The product was analyzed with ^1H NMR, ^{13}C NMR and LCMS. ^1H NMR (400MHz, DMSO) δ : 1.13 (t, $J = 7.1$, 3H), 1.41 (t, $J = 7.3$, 3H), 2.05 (quint, $J = 7.2$, 2H), 2.35 (t, $J = 7.5$, 2H), 4.00 (q, $J = 7.1$, 2H), 4.24 (q, $J = 7.3$, 2H), 4.28 (t, $J = 6.8$, 2H), 7.93-7.94 (d, $J = 1.2$ 1H), 7.95-7.96 (d, $J = 1.2$ 1H),

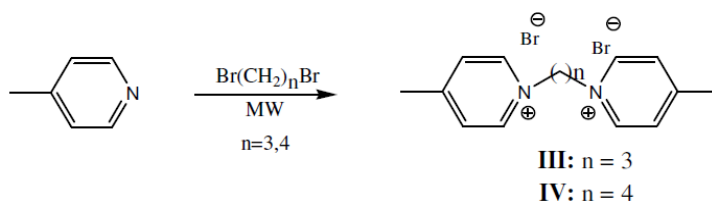
9.57 (s, 1H); ^{13}C NMR (100MHz, DMSO) δ : 14.0 (CH₃), 15.0 (CH₃), 24.9 (CH₂), 30.1 (CH₂), 44.1 (CH₂), 47.9 (CH₂), 59.9 (CH₂), 122.1 (CH), 122.3 (CH), 135.9 (CH), 171.8 (C); LCMS: m/z 211 (M⁺).

1-ethyl-3-phenethylimidazol-3-ium bromide (II)

N-ethylimidazole (1 g, 0.0104 mol), (2-bromoethyl) benzene (1.92 g, 0.0104 mol) and 10 mL of toluene were placed in a microwave reactor vessel and irradiated for 20 minutes at 100 °C. The crude product was washed a few times with dry ethyl acetate and dried overnight in a vacuum at 70 °C. The yield of **II** was 91%. The product was analyzed with ^1H NMR, ^{13}C NMR and LCMS. ^1H NMR (400MHz, DMSO) δ : 1.37 (t, $J = 7.3$, 3H), 3.17 (t, $J = 7.2$, 2H), 4.19 (q, $J = 7.4$, 2H), 4.48 (t, $J = 7.4$, 2H), 7.18-7.34 (m, 5H), 7.85-7.86 (m, 1H), 7.86-7.87 (m, 1H), 9.33 (s, 1H); ^{13}C NMR (100MHz, DMSO) δ : 15.2 (CH₃), 35.6 (CH₂), 44.1 (CH₂), 49.8 (CH₂), 122.0 (CH), 122.4 (CH), 126.8 (CH), 128.5(CH), 128.7(CH), 135.7(CH), 136.9 (C); LCMS: m/z 201 (M⁺).

Microwave assisted synthesis of pyridinium ionic liquids

Although compounds **III** and **IV** have been previously reported by conventional methods [23], their preparation under microwave irradiation has never been disclosed.



Scheme 2. Synthesis of pyridinium-based ionic liquids under microwave irradiation (MW).

1,1'-(propane-1,3-diyl)bis(4-methylpyridinium)dibromide (III)

4-picoline (2 g, 0.0215 mol), 1,3-dibromopropane (2.1 g, 0.0107 mol) and 10 mL of toluene were placed in a microwave reactor vessel and irradiated for 20 minutes at 100 °C. The crude product was washed a few times with dry ethyl acetate and dried overnight in a vacuum at 70 °C. The yield of **III** was 90%. The product was analyzed with ^1H NMR, ^{13}C NMR and LCMS. ^1H NMR (400MHz, DMSO) δ : 2.6 (s, 6H), 2.65 (quint, $J = 7.3$, 2H), 4.73 (t, $J = 7.5$, 4H), 8.03 (d, $J = 6.6$ 4H), 9.05 (d, $J = 6.6$ 4H); ^{13}C NMR (100MHz, DMSO) δ : 21.4 (CH₃), 31.7 (CH₂), 56.6 (CH₂), 128.4 (CH), 143.9 (CH), 159.1 (C).

1,1'-(butane-1,3-diyl)bis(4-methylpyridinium)dibromide (IV)

4-picoline (2 g, 0.0215 mol), 1,4-dibromopropane (2.31 g, 0.0107 mol) and 10 mL of toluene were placed in a microwave reactor vessel and irradiated for 20 minutes at 100 °C. The crude product was washed a few times with dry ethyl acetate and dried overnight in a vacuum at 70 °C. The yield of **IV** was 92%. The product was analyzed with ^1H NMR, ^{13}C NMR and LCMS. ^1H NMR (400MHz, DMSO) δ : 1.92 (m, 4H), 2.59 (s, 6H), 4.58 (m, 4H), 7.95 (d, $J = 6.8$ 4H), 8.88 (d,

$J = 6.8 \text{ 4H}$); ^{13}C NMR (100MHz, DMSO) δ : 21.6 (CH_3), 27.3 (CH_2), 59.4 (CH_2), 128.7 (CH), 143.8 (CH), 159.3 (C).

Electrochemical tests

For the weight loss measurements, carbon steel sheets of 4 cm^2 size, and of chemical composition (wt%): C = 0.15%, Mn = 0.45%, Si = 0.10, S = 0.05%, P% = 0.03% and the remainder Fe, were used. The samples were abraded with a series of emery papers, from a coarse grade 500 and proceeding in steps to fine grade 1500, washed thoroughly with doubly distilled water. The cleaned samples were weighed before and after immersion in 1.0 M HCl for 4 hours in the absence and presence of various concentrations of the four ILs inhibitors.

The potentiodynamic polarization experiments were carried out in a conventional three-electrode electrochemical cell. A carbon steel cylinder pressed into a Teflon holder acted as a working electrode (WE). Its working area of 0.5 cm^2 remained precisely fixed. A saturated calomel electrode (SCE) connected through a salt bridge was used as a reference electrode, while a platinum wire was used as a counter electrode. The electrode was abraded similar to that mentioned above.

Electrochemical measurements were performed using a potentiostat/galvanostat SI 1287 Solartron, software packages CorrWare 2, and CorrView 2 provided by Solartron were used to obtain the polarization curves.

The polarization curves were recorded by changing the electrode potential automatically from ca. -0.95 V to -0.75 V with a scan rate of 20 mVs^{-1} . From polarization curves measured using only the range $\pm 10 \text{ mV}$ before and after E_{corr} , with scan rate of 1.0 mV s^{-1} , the polarization resistance R_p was evaluated. All of the experiments were triplicate to ensure reproducibility.

Results and discussion

Weight loss studies

The weight loss of steel in 1.0 M HCl in the absence and presence of various concentrations ($1 \times 10^{-4} - 5 \times 10^{-3} \text{ M}$) of the four ILs were obtained after 4 h of immersion at $25 \text{ }^\circ\text{C}$. Eq. (1) determines the inhibition efficiency:

$$\eta_{\text{WL}}\% = (1 - W_{\text{inh}} / W) \times 100 \quad (1)$$

where W and W_{inh} are the weight loss of steel in the absence and presence of the inhibitors, respectively. The results of the four tested ILs compounds in Table 2 showed that the $\eta_{\text{WL}}\%$ increases with increase in the concentration of the inhibitors. Based on the maximum inhibition efficiency, the inhibitors can be ranked as follows: II > III > I > IV.

Table 2. Inhibition efficiencies for various concentrations of compounds I, II, III and IV for the corrosion of C-steel in 1.0 M HCl from weight loss measurements.

Concentration (mol dm ⁻³)	$\eta_{WL}\%$
1 M HCl (blank)	-
Compound I	
1 × 10 ⁻⁴	36.0
5 × 10 ⁻⁴	40.0
1 × 10 ⁻³	61.9
5 × 10 ⁻³	71.1
Compound II	
1 × 10 ⁻⁴	31.9
5 × 10 ⁻⁴	47.5
1 × 10 ⁻³	64.1
5 × 10 ⁻³	80.9
Compound III	
1 × 10 ⁻⁴	47.5
5 × 10 ⁻⁴	62.5
1 × 10 ⁻³	73.3
5 × 10 ⁻³	80.0
Compound IV	
1 × 10 ⁻⁴	50.8
5 × 10 ⁻⁴	55.6
1 × 10 ⁻³	64.5
5 × 10 ⁻³	71.3

Table 3. Electrochemical parameters for C-steel in 1.0 M HCl obtained from the polarization curves at different ILs inhibitor concentrations.

Concentration (mol dm ⁻³)	j_{corr} (A/cm ²)	$-E_{corr}$ (mV)	β_a (mV/dec)	β_c (mV/dec)	$\eta_{pol}\%$	C.R. (mpy)
1 M HCl (blank)	0.0040100	847.70	181.3	317.4	-	1835.3
Compound I						
1 × 10 ⁻⁴	0.00253	859.6	144.0	208.5	36.9	1157.6
5 × 10 ⁻⁴	0.00247	858.6	151.7	155.3	38.3	1132.8
1 × 10 ⁻³	0.00143	861.5	127.6	172.6	64.3	656.3
5 × 10 ⁻³	0.00111	859.5	110.2	142	72.3	509.2
Compound II						
1 × 10 ⁻⁴	0.002796	825.4	139.9	165.8	30.3	1279.8
5 × 10 ⁻⁴	0.0021855	847.8	145.9	212.9	45.5	1000.3
1 × 10 ⁻³	0.0015220	834.7	87.6	115.4	62.0	696.6
5 × 10 ⁻³	0.0008115	826.6	164.9	146.0	79.8	371.4
Compound III						
1 × 10 ⁻⁴	0.0021620	837.7	143.1	192.5	46.1	989.5
5 × 10 ⁻⁴	0.0014560	837.9	102.7	163.7	63.8	666.4
1 × 10 ⁻³	0.0010311	817.0	157.8	211.7	74.0	471.9
5 × 10 ⁻³	0.0008428	821.2	84.3	140.6	79.0	385.7
Compound IV						
1 × 10 ⁻⁴	0.0020383	832.6	108.5	187.8	49.2	932.9
5 × 10 ⁻⁴	0.0019172	827.5	104.0	180.0	52.2	877.5
1 × 10 ⁻³	0.0014519	829.4	119.4	199.3	63.8	664.5
5 × 10 ⁻³	0.0012158	822.4	124.2	149.3	70.0	556.5

Potentiodynamic polarization curves

Tafel plots for steel in 1.0 M HCl solution with and without various concentrations of the four ILs are shown in Figs. 1-4. Various kinetic data and corrosion parameters such as corrosion potential (E_{corr}), corrosion current density

(j_{corr}), cathodic and anodic Tafel slopes (β_c , β_a), corrosion rate (CR) in mpy and the inhibition efficiency ($\eta_{\text{pol}}\%$) are listed and summarized in Table 3. Corrosion current densities were obtained by linear extrapolation of the anodic and cathodic branches of the Tafel plots to the corrosion potential. The corrosion rate is determined in mils per year (mpy) using: $\text{CR} = 0.129 a / n D$ [24], where CR is the corrosion rate in mpy, a is the atomic weight of the metal, n is the number of electrons in the reduction of the metal ions, D is the density of the metal in g/cm^3 , and j is the corrosion current density in $\mu\text{A/cm}^2$.

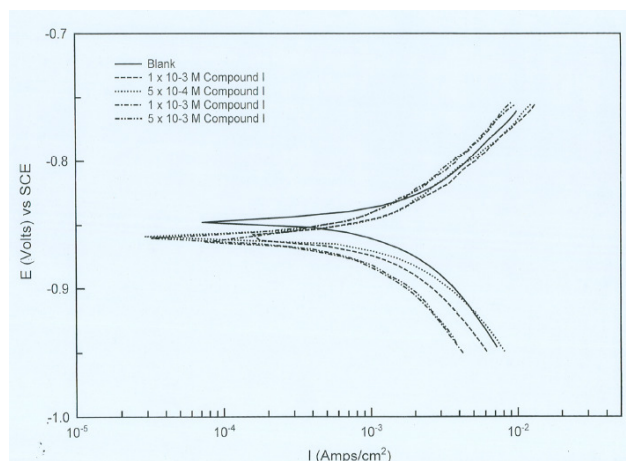


Figure 1. Potentiodynamic cathodic and anodic polarization scans for C-steel in 1.0 M HCl in the absence and presence of different concentrations of compound I.

Fig. 1 represents the influence of various concentrations of compound I on the polarization behavior of steel in 1.0 M HCl. In this case, the cathodic branch of the polarization curve is more affected by the addition of the inhibitor than the anodic branch. In addition, the corrosion potential in solutions containing inhibitor is shifted towards more negative values with increase of the inhibitor concentrations. This indicates that this compound acts as a mixed type inhibitor with predominant cathodic.

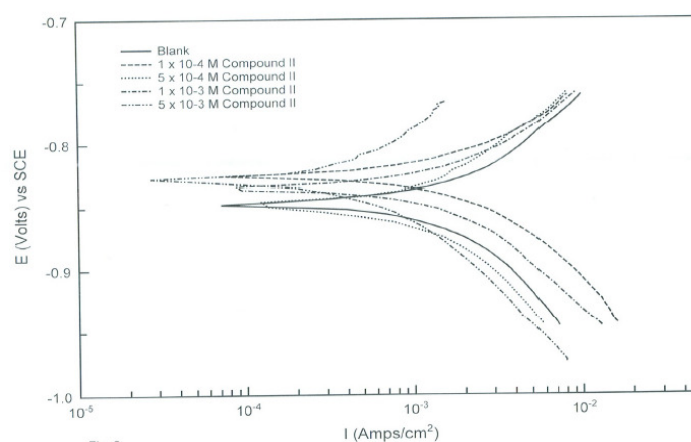


Figure 2. Potentiodynamic cathodic and anodic polarization scans for C-steel in 1.0 M HCl in the absence and presence of different concentrations of compound II.

Fig. 2 represents the influence of various concentrations of compound II on the polarization behavior of steel in 1.0 M HCl. The anodic current decreased with increasing the inhibitor concentration and the corrosion potential is shifted to more positive potential indicating a mixed type inhibitor with predominant anodic. According to some researchers [25,26], an inhibitor behaves as anodic or cathodic only if displacement due to inhibitor addition is at least of 85 mV with respect to E_{corr} of the blank solution (absence of the inhibitor). In the present case, (compounds I and II) shift were lower than the referenced value, which suggests that experimental compounds can be defined only as mixed type inhibitors with predominant anodic.

The inhibition efficiency $\eta_{\text{pol}}\%$ at different inhibitor concentrations was calculated from the following equation:

$$\eta_{\text{pol}}\% = (1 - j_{\text{corr}} / j_{\text{corr}}^0) \times 100 \quad (2)$$

where j_{corr} and j_{corr}^0 are the current density in the absence and presence of inhibitors, respectively. The $\eta_{\text{pol}}\%$ increases with increasing the concentration of the inhibitors. The results suggest the inhibitor molecules are adsorbed at the steel/solution interface where the adsorbed molecules partly hinder the active sites of the corrodent. The increase in $\eta_{\text{pol}}\%$ observed at higher inhibitor concentration indicates that the adsorption process enhances with increasing inhibitor concentration, which leads more inhibitor molecules to adsorb on the metal surface, thus resulting large surface coverage.

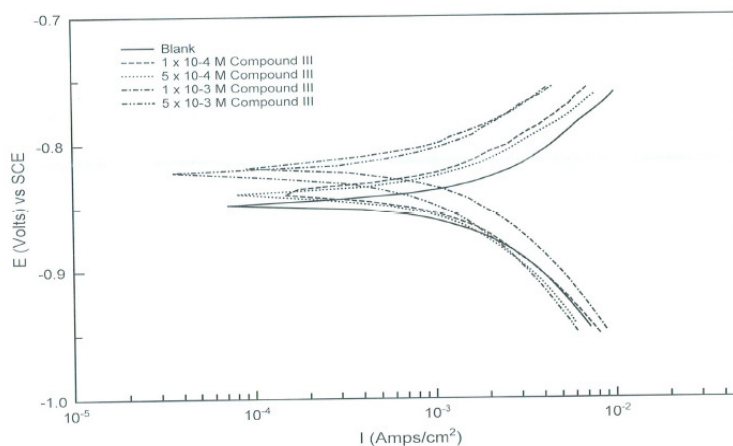


Figure 3. Potentiodynamic cathodic and anodic polarization scans for C-steel in 1.0 M HCl in the absence and presence of different concentrations of compound III.

Figs. 3 and 4 represent the influence of adding various concentrations of compound III and compound IV, respectively, on the polarization behavior of steel in 1.0 M HCl. It is observed that the presence of ionic liquid affected both the anodic dissolution of steel and the cathodic hydrogen evolution reaction in 1.0 M HCl. These compounds decreased the corrosion current density and shifted E_{corr} towards more noble potential values, indicating that the inhibitors act as mixed type.

It is of practical importance to study the inhibitor behavior at higher temperatures since the pickling of the steel is run at temperatures up to 60 °C. The effect of temperature on the corrosion behavior of steel in presence of 1×10^{-3} M of compound II was studied in the temperature range 298-338 K as a representative example using the three different techniques. The electrochemical parameters again were collected at Table 4. The results showed an increase in the inhibition efficiency with raising the solution temperature. This indicates physical adsorption of the inhibitors. The inhibition efficiency was found to increase with raising the solution temperature. This could be explained by the fact that at high temperatures the surface covered by the inhibitor increases and the rate determining step of the metal dissolution becomes the diffusion through the film of corrosion products and inhibitor. Inspection of the data reveals that an increase of temperature shifts the values of E_{corr} to more negative potentials. The values of j_{corr} increase with increasing temperature as a result of the higher dissolution of the metal at higher temperatures. The thermodynamic functions for the dissolution of steel in 1.0 M HCl in the absence and presence of compound II were obtained by applying the Arrhenius equation (3) and transition state equation (4), respectively, and the results are given in Table 5:

$$\log j_{\text{corr}} = (-E_a / 2.303 RT) + \lambda \quad (3)$$

$$j_{\text{corr}} = RT/Nh \exp (\Delta S_a / R) \exp (\Delta H_a / RT) \quad (4)$$

where E_a is the apparent activation energy, R is the universal gas constant, λ is the Arrhenius pre-exponential factor, ΔS_a is the change in entropy of activation, ΔH_a is the change in enthalpy of activation, h is Planck's constant and N is the Avogadro's number. According to eq. (3), the apparent activation energy E_a can be obtained by plotting $\log (j_{\text{corr}})$ against $1/T$ (Fig. 5). However, a plot of $\log (j_{\text{corr}}/T)$ against $1/T$ according to eq. (4) should give straight line with a slope of $(-\Delta H_a / 2.303 R)$ and an intercept of $(\log R/Nh + \Delta S_a / 2.303 R)$, as shown in Fig. 6. The value of the activation energy for the inhibited process is determined at the highest concentrations used, in order to assure that the achieved coverage degree is close to the maximal value. The activation energy, E_a , in case of steel, was found to be 46.9 kJ mol⁻¹, in absence, and 29.9 kJ mol⁻¹, in presence, of compound II. The value of the activation energy in presence of inhibitor is lower than in 1 M HCl. Similar result of decreasing activation energy in presence of inhibitors has been previously reported by Popova et al. [27]. The pre-exponential factor in the Arrhenius equation, λ , for heterogeneous reaction, is related to the number of active centers [28]. These active centers have different energy, if energetic surface heterogeneity is assumed. There are two possibilities: in the first case ($E_{a,\text{inh}}$ is greater than $E_{a,\text{HCl}}$) the inhibitor is adsorbed on the most active adsorption sites (having the lowest energy) and the corrosion process takes place predominantly on the active sites of the higher energy. In the second case ($E_{a,\text{inh}}$ is lower than $E_{a,\text{HCl}}$), observed in these experiments, the value of λ is lower ($\lambda = 4.46 \times 10^{-3}$) than that in pure HCl ($\lambda = 0.0316$), i.e., a smaller number of more active sites remain uncovered which take part in the corrosion process [29].

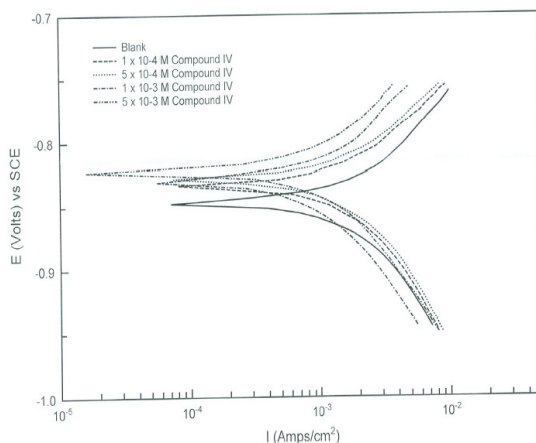


Figure 4. Potentiodynamic cathodic and anodic polarization scans for C-steel in 1.0 M HCl in the absence and presence of different concentrations of compound IV.

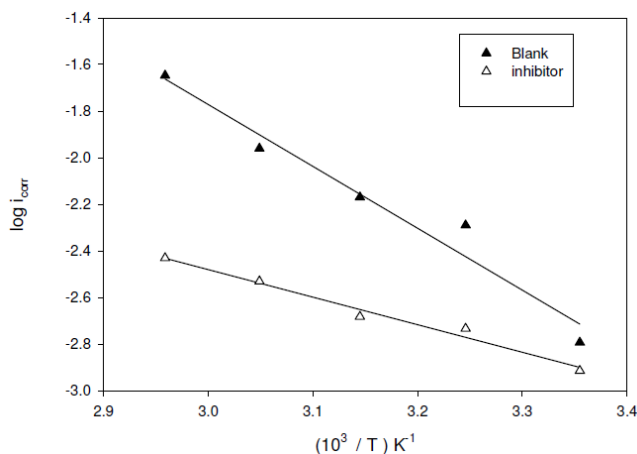


Figure 5. Arrhenius plots for C-steel in 1 M HCl solution in the absence and presence of 1×10^{-3} M of compound II.

Table 4. Effect of temperature on the electrochemical parameters and the inhibition efficiencies in presence of 1×10^{-3} M of compound II determined from potentiodynamic polarization curves, linear polarization and weight loss methods.

T / K	Blank			Blank + 1×10^{-3} M Compound II			$\eta_{pol}\%$	$\eta_{Rp}\%$	$\eta_{WL}\%$
	j_{corr} (A/cm ²)	$-E_{corr}$ (mV)	R_p (Ω/cm^2)	j_{corr} (A/cm ²)	$-E_{corr}$ (mV)	R_p (Ω/cm^2)			
298	0.0016149	835.8	18.6	0.0012176	832.7	23.4	24.6	25.8	26.5
308	0.0051448	877.9	11.6	0.0018486	864.4	18.9	64.1	62.9	65.7
318	0.006769	881.1	9.5	0.0020797	873.8	16.0	69.2	68.4	69.9
328	0.0069829	888.1	7.9	0.002025	878.7	13.5	71.0	70.9	71.5
338	0.022523	895.2	5.9	0.005790	887.9	10.3	74.0	74.6	75.9

Table 5. Thermodynamic parameters for C-steel in 1 M HCl obtained from polarization measurements in presence of 1×10^{-3} M of compound II.

$-\Delta S_a$ (J mol ⁻¹)	ΔH_a (kJ mol ⁻¹)	E_a (kJ mol ⁻¹)
232.6	49.1	46.9
132.7	20.0	29.9

Blank
Compound II

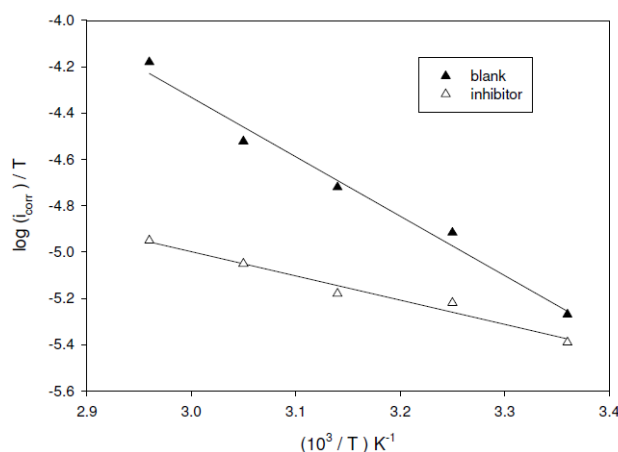


Figure 6. Plot of $(\log i_{corr})/T$ vs. $10^3/T$ for C-steel in 1 M HCl in the absence and presence of 1×10^{-3} M of compound II.

The entropy of activation ΔS_a in the absence and presence of compound II is large and negative (Table 5). This implies that the activated complex in the rate determining step represents an association rather than a dissociation step, meaning that a decrease in disordering takes place on going from reactants to the activated complex [30]. The value of ΔH_a reflects the strong adsorbability of the tested compound on the steel surface and indicates the endothermic nature of the process.

Linear polarization measurements

In order to determine the polarization resistance, R_p , the working electrode was polarized ± 10 mV in the vicinity of the corrosion potential at a scan rate of 1 mVs^{-1} . The polarization resistance values were determined from the slope of the current density-potential lines

$$R_p = A \, dE / dj \quad (5)$$

where A is the surface area of the electrode, dE is the change in potential and dj is the change in current. The R_p values were used to calculate the inhibition efficiencies, $(\eta_{Rp} \%)$ using the relationship:

$$\eta_{Rp} \% = (1 - R_p / R_p^0) \times 100 \quad (6)$$

where R_p and R_p^0 are the polarization resistance in the absence and presence of inhibitors, respectively. From Table 6, it can be seen that by increasing the inhibitor concentration, both the polarization resistance and the inhibition efficiency increase, indicating adsorption of the inhibitors on the metal surface to block the active sites and inhibit corrosion. The inhibition efficiency again is seen to decrease in the following order, II > III > I > IV.

Obtained results from Tafel polarization, linear polarization and weight loss are in good agreement with each other.

Table 6. Polarization resistances and inhibition efficiencies obtained from the linear polarization method for C-steel in 1.0 M HCl.

Concentration (mol dm ⁻³)	R _p (Ω/ cm ²)	η _{Rp} %	Concentration (mol dm ⁻³)	R _p (Ω/ cm ²)	η _{Rp} %
1 M HCl (blank)	11.6	-	Compound III		
Compound I			1 × 10 ⁻⁴	16.8	44.8
1 × 10 ⁻⁴	16.0	37.9	5 × 10 ⁻⁴	18.8	62.1
5 × 10 ⁻⁴	16.2	39.6	1 × 10 ⁻³	20.1	73.3
1 × 10 ⁻³	18.9	62.9	5 × 10 ⁻³	20.8	79.3
5 × 10 ⁻³	19.8	70.7	Compound IV		
Compound II			1 × 10 ⁻⁴	17.2	48.3
1 × 10 ⁻⁴	15	29.3	5 × 10 ⁻⁴	17.9	54.3
5 × 10 ⁻⁴	16.8	44.8	1 × 10 ⁻³	18.7	61.2
1 × 10 ⁻³	18.6	60.3	5 × 10 ⁻³	19.7	69.8
5 × 10 ⁻³	20.9	79.9			

Adsorption isotherm

Basic information dealing with the interaction between the inhibitor molecules and the metal surface can be provided by adsorption isotherms [31]. In order to get more knowledge about the mode of adsorption of ILs on the surface of the steel, the data obtained from the potentiodynamic polarization curves have been tested with the well known adsorption isotherms. Data obtained from polarization measurements were tested graphically for fitting various isotherms including Langmuir, Frumkin and Temkin. Among these isotherms, the best fit was obtained with the Langmuir isotherm. According to this isotherm Θ is related to the inhibitor concentration by the following equation:

$$c / \Theta = (1 / K_{\text{ads}}) + c \quad (7)$$

where c is the inhibitor concentration in mol dm⁻³, Θ is the degree of surface coverage ($\theta = \eta / 100$) and K_{ads} is the equilibrium constants of adsorption process. It is noted that the straight lines obtained on plotting c / Θ vs. c , as shown in Fig.7, suggest that the adsorption of the ILs inhibitors on the steel surface in HCl solution follows Langmuir's adsorption isotherm. The degree of surface coverage was found to increase with increasing the concentration of additive.

The free energy of adsorption (ΔG_{ads}) was calculated from the equation [32]:

$$\Delta G_{\text{ads}} = -RT \ln (55.5 K_{\text{ads}}) \quad (8)$$

where 55.5 mol dm⁻³ is the molar concentration of water in the solution, R is the gas constant and T is the absolute temperature. Generally, values of ΔG_{ads} up to -20 kJ mol⁻¹ are consistent with electrostatic interactions between the charged molecules and the charged metal (physisorption), while those around -40 kJ mol⁻¹ or higher are associated with chemisorption as a result of sharing or transfer of electrons from ILs molecules to the metal surface to form a coordinate type of bond (chemisorption) [33]. The absolute values of ΔG_{ads} calculated in presence of the four ILs inhibitors are found to be relatively small (around 30 kJmol⁻¹).

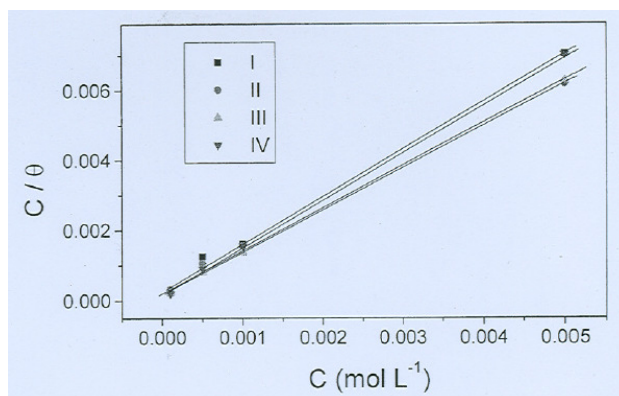


Figure 7. Langmuir isotherm for the adsorption of compounds I, II, III and IV by using Tafel polarization method.

Therefore, the results indicate the inhibitors to be physically adsorbed on the surface and their negative sign indicates spontaneous interaction of inhibitor molecule with the corroding steel surface [34]. In general, all the inhibitors used in this study have two nitrogen atoms in their molecular structure. These two nitrogen atoms could be in one ring, e.g., imidazolium compounds (I and II) or in two different rings, e.g., pyridinium compounds (compounds III and IV). Adsorption can occur through the formation of an iron-nitrogen coordinate bond or π -electron interaction between the heterocyclic in their molecules with aromatic character and the iron substrate. Adsorption can also occur via electrostatic interactions between a negatively charged surface (due to the specific adsorption of Br^- anion on the steel surface) and the positive charge of the cationic molecules. In addition, electrostatic interactions could be achieved due to the ionic liquid compounds and the solid surfaces which can play a role in the adsorption process. Comparing compounds I and II, the latter is characterized by the presence of benzene ring instead of $-\text{CH}_2-\text{COEt}$ group in compound I. Therefore, compound II has a higher rate of relaxation of the adsorbed inhibitors from the metal surface because of the flat aromatic head groups that can π -back bond with Fe^{2+} .

In the case of compounds III and IV, i.e., pyridinium compounds, it was found that shorter chain for pyridinium compounds (Compound III) raised values of Θ and consequently $\eta\%$. The compound of pyridinium participates in a more parallel rather than perpendicular orientation at the surface, due to the presence of two flat aromatic head groups that can π -back bond with Fe^{2+} . Thus, the adsorbed molecule would occupy a larger surface area compared with a perpendicular orientation which is the reason for high $\eta\%$ of compound III in comparison with compound IV.

Surface morphology study

The surface morphologies of C-steel specimen in 1.0 M HCl solution free or containing some of the ILs inhibitors after 4 h immersion were examined using scanning electron microscopy (SEM), as displayed in Fig. 8a–c. In the absence of inhibitors (Fig. 8a), a very rough surface was observed due to rapid corrosion attack of carbon steel by chloride anions. There are a large number of pits

surrounded by iron oxide layer which almost fully covers the carbon steel surface, revealing that pit formation under these conditions occurs continuously during the exposure period while iron oxide builds up over the surface. It is important to stress out that when ILs inhibitors (II and III) are present in the solution (Fig. 8b,c), the morphology of the carbon steel surface is quite different from the previous one and the rough surface (amount of the formed iron oxide and the number of pits) is visibly reduced, indicating the formation of a protective film.

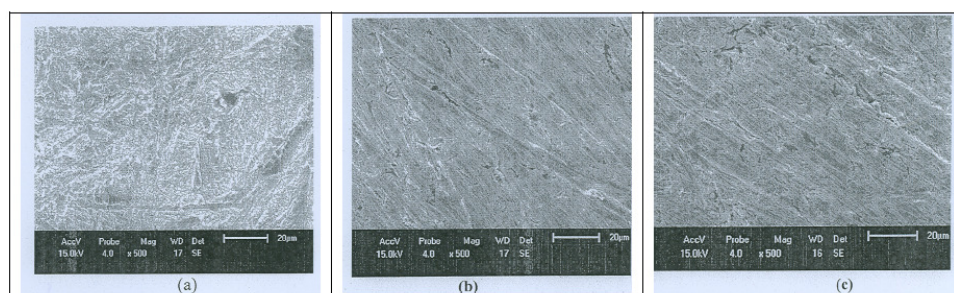


Figure 8. SEM micrographs of the surface of the C-steel specimens in 1.0 M HCl in absence (a), and in presence of 1×10^{-3} M of compound II (b) and 1×10^{-3} M of III (c).

Conclusion

From the overall experimental results and discussion the following conclusions can be deduced:

- The four tested ILs behave as inhibitors for the corrosion of the C-steel in 1 M HCl solution.
- The inhibition efficiency increased with increasing the inhibitor concentration. All of the ILs act as mixed-type inhibitors.
- The inhibition is due to the adsorption of the inhibitor molecules on the C-steel surface and the blocking of active sites.
- Obtained results from Tafel polarization, linear polarization and weight loss are in good agreement with each other.
- The adsorption of the four ILs inhibitors obeys the Langmuir adsorption isotherm.

Acknowledgements

The authors gratefully acknowledge the financial support from Taibah University (Grant 430/417).

References

1. I. Ahamad, C. Gupta, R. Prasad, M.A. Quraishi, *J. Appl. Electrochem.* 40 (2010) 2171.
2. F. El-Taib Heikal, A.S. Fouda and M.S. Radwan, *Mater. Chem. Phys.* 125 (2011) 26.

3. B. Mernari, H. Elattari, M. Traisnel, F. Bentiss, M. Lagrenee, *Corrosion* 40 (1998) 391.
4. S.S. Abd El Rehim, Magdy A.M. Ibrahim, K.F. Khaled, *Mater. Chem. Phys.* 70 (2001) 268.
5. M.M. Hamza, S.S. Abd El Rehim and Magdy A.M. Ibrahim, *Arab. J. Chem.* (in press).
6. S.S. Abd El Rehim, Magdy A.M. Ibrahim and K.F. Khaled, *J. Appl. Electrochem.* 29 (1999) 593.
7. K.F. Khaled, A.El-mghraby, O.B. Ibrahim, O.A. Elhabib, Magdy A.M. Ibrahim, *J. Mater. Environ. Sci.* 1(3) (2010) 139.
8. I. Sekine, Y. Nakata, H. Tanabe, *Corros. Sci.* 28 (1988) 987.
9. A. Popova, M. Christov, S. Raicheva, E. Sokolova, *Corros. Sci.* 46 (2004) 1333.
10. A. Popova, M. Christov, T. Deligeorgiev, *Corrosion* 59 (2003) 756.
11. A. Popova, E. Sokolova, S. Raicheva, M. Christov, *Corros. Sci.* 45 (2003) 33.
12. A. Popova, M. Christov, *Corros. Sci.* 48 (2006) 3208.
13. T. Tsuda, C.L. Hussey, *Interface* 16 (2007) 42.
14. S. Zhang, N. Sun, X. He, X. Lu, X. Zhang, *J. Phys. Chem. Ref. Data* 35 (2006) 4.
15. H. Zhao, *Chem. Eng. Comm.* 193 (2006) 1660.
16. H. Ashassi-Sorkhabi, M. Es'haghi, *Mater. Chem. Phys.* 114 (2009) 267.
17. N.V. Likhanova, M.A. Dominguez-Aguilar, O. Olivares-Xometl, N. Nava-Entzana, E. Arce, H. Dorantes, *Corros. Sci.* 52 (2010) 2088.
18. Q.B. Zhang, Y. X. Hua, *Electrochim Acta* 54 (2009) 1881.
19. R. Gasparac, C.R. Martin, E. Stupnisek-lisek, *J. Electrochem. Soc.* 147 (2000) 548.
20. S. Muralidharan, S.V.K. Lyer, *Anti-Corros. Methods Mater.* 44 (1997) 100.
21. M.E. Palomar, C.O. Olivares-Xometl, N.V. Likhanova, J.B. Perez-Navarrete, *J. Surfact. Deterg.* 14 (2011) 211.
22. M.A. Quraishi, M.Z.A. Rafique, S. Khan, N. Saxena, *J. Appl Electrochem.* 37 (2007) 1153.
23. J. Beata, K. Janina, P. Jerzy, *Dyes and Pigments* 73(3) (2006) 361.
24. Sk.A. Ali, M.T. Saeed, S.U. Rahman, *Corros. Sci.* 45 (2003) 253.
25. M.M. Saleh, A.A. Atia, *J. Appl. Electrochem.* 36 (2006) 899.
26. E.S. Ferreira, C. Giacomelli, F.C. Giacomelli, A. Spinelli, *Mater. Chem. Phys.* 83 (2004) 129.
27. A. Popova, M. Christov, *Corros. Sci.* 48 (2006) 3208.
28. P.W. Atkins, *Physical Chemistry*, Mir, Moscow, 1980.
29. A. Popova, M. Christov, A. Vasilev, *Corros. Sci.* 49 (2007) 3276.
30. M.K. Gomma, M.H. Wahdan, *Mater. Chem. Phys.* 39 (1995) 209.
31. E. McCafferty, in: H. Leidheister Jr. (Ed.), *Corrosion Control by Coating*, Science Press, Princeton, 1979, p. 279.
32. J.M. Cases, F. Villieras, *Langmuir* 8 (1992) 1251.
33. S.A. Umoren, E.E. Ebenso, *Mater. Chem. Phys.* 106 (2007) 393.
34. M. Abdullah, *Corros. Sci.* 44 (2002) 717.